

Quantum liquid crystals in strongly correlated materials and ultracold gases

Nathaniel Burdick

December 13, 2010

Abstract

Classical liquid crystal phases are characterized by broken symmetries. Phases within strongly correlated materials that break similar symmetries have been predicted and observed, and systems exhibiting such phases have been deemed quantum liquid crystals (QLC). This paper presents the existence of QLC behavior in the quantum Hall system GaAs/GaAlAs, the strontium ruthenate $\text{Sr}_3\text{Ru}_2\text{O}_7$, and arguably the cuprate superconductor $\text{YBa}_2\text{Cu}_3\text{O}_{6+x}$, as well as the possibility of producing QLC phases in ultracold dipolar gases.

1 Introduction

In 1991, Pierre-Gilles de Gennes was awarded the Nobel Prize in Physics for his work with liquid crystals, which has blossomed into a beautiful and fruitful field. Liquid crystal theory has since found a surprising application outside the classical interactions of elongated (and other oddly-shaped) molecules and has been used to study and understand strongly correlated electronic systems. First proposed in 1998 [1], the resultant class of systems have been deemed “electronic liquid crystals” or “quantum liquid crystals.” Quantum liquid crystal (QLC) theory offers an alternative to Fermi liquid theory and may even offer an explanation (or partial explanation) of the pseudogap in high- T_C superconductors, a region where Fermi liquid theory has generally failed [2].

Quantum liquid crystals are characterized by a phase or series of phases that exhibit the same symmetry breaking observed in classical liquid crystal phases: The nematic phase maintain translational symmetry but break a rotational symmetry; the smectic phases break a degree of translational symmetry (forming stripes) as well as rotational symmetry. Remarkably, while classical liquid crystals are made up of objects that already break symmetry (i.e., objects that are elongated, discoid, helical, etc.), QLCs are composed of electrons, which are point-like particles [3]. Thus, though the observed phases are analogous, the mechanisms behind those phases are very different between classical and quantum liquid crystals.

In Sec. 2 of this paper, some basic treatment of classical liquid crystals will be presented, followed by the extension to quantum liquid crystals. Discussion will then turn to three sources of experimental evidence for QLC phases in strongly correlated materials (Sec. 3): the quantum Hall system GaAs/GaAlAs, the strontium ruthenate $\text{Sr}_3\text{Ru}_2\text{O}_7$, and the cuprate superconductor $\text{YBa}_2\text{Cu}_3\text{O}_{6+x}$. Finally, proposals for producing QLC phases in ultracold gases will be discussed in Sec. 4.

2 Liquid crystal theory

2.1 Classical liquid crystals

While other liquid crystal phases exist, the two most relevant to strongly correlated systems are the nematic phase and smectic phase¹. Both phases will be discussed, though the nematic will receive greater attention.

2.1.1 Nematic phases

As mentioned above, the nematic phase is spatially uniform (i.e., preserves translational symmetry) but anisotropic (i.e., breaks rotational symmetry). Figure 1(a) is a depiction of the nematic phase. In the case of elongated molecules, the molecules align their orientations but do not spatially order their centers of mass. The direction of alignment, \mathbf{n} , is defined as the nematic axis. The distribution of particles in conventional nematics has two general properties [4]:

¹In actuality, the smectic phase is comprised of three phases: smectic A, hexatic smectic B, and smectic C. The distinction between these three phases is not relevant to this paper, however.

1. The distribution is symmetric about \mathbf{n} .
2. The distribution does not distinguish between \mathbf{n} or $-\mathbf{n}$.

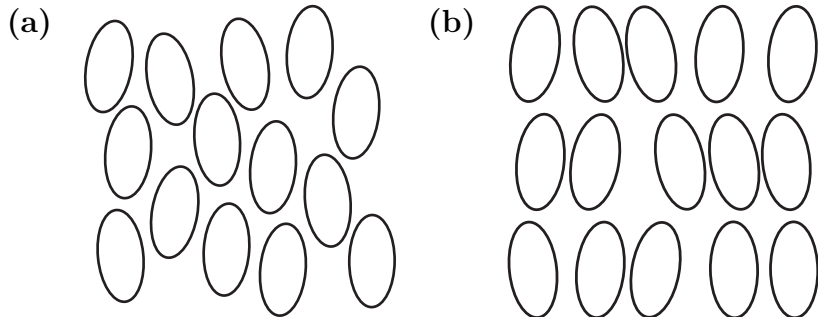


Figure 1. (a) A depiction of the nematic phase. The centers of mass have no spatial ordering, but the molecules orient themselves along a single axis defined as the nematic axis, breaking one degree of rotational symmetry. (b) A depiction of a smectic phase. Smectic phases break rotational symmetry as well as translational symmetry, forming layers.

The first condition dictates that the nematic order parameter does not depend the azimuthal angle, ϕ . The second causes the average over θ , $\langle \cos \theta \rangle$, to vanish. Thus, the simplest and most natural order parameter is

$$S \equiv \left\langle \frac{3 \cos^2 \theta - 1}{2} \right\rangle. \quad (1)$$

In assigning an experimentally measurable quantity to the order parameter, any traceless, symmetric tensor satisfies (1) and is appropriate [4].

2.1.2 Smectic phases

In addition to the rotational symmetry broken by the nematic phase, the smectic phases break one degree of translational symmetry. The molecules form layers with well-defined spacing, d , such that the liquid is no longer uniform. The natural axis defined by smectics is the normal vector, \mathbf{z} , of the layers. Figure 1(b) is a depiction of the smectic A phase in which the molecules align along \mathbf{z} . Other configurations are possible, such as the smectic C phase in which the molecules align at some angle with \mathbf{z} [4].

For the purposes of this paper, only “smectic order” need be considered, which refers to the layering observed in smectic phases. Thus, the normal vector, \mathbf{z} , and interlayer spacing, d , is sufficient, and no formal treatment of a smectic order parameter will be given.

2.2 Quantum liquid crystals

2.2.1 Nematic phases

The following treatment of the QLC nematic phase comes from [5] in which Oganesyanyan *et al.* first developed the theory of a nematic Fermi fluid. The simplest case considered is a

two-dimensional system of spinless fermions. Because the result for classical liquid crystals (1) only depends on symmetry considerations, the same holds true for the QLC nematic, and any traceless, symmetric tensor can serve as the order parameter. Oganessian *et al.* take the order parameter to be the quadrupole density:

$$\hat{\mathbf{Q}}(x) \equiv -\frac{1}{k_F^2} \Psi^\dagger(\mathbf{r}) \begin{pmatrix} \partial_x^2 - \partial_y^2 & 2\partial_x\partial_y \\ 2\partial_x\partial_y & \partial_y^2 - \partial_x^2 \end{pmatrix} \Psi(\mathbf{r}), \quad \text{where } B > 0. \quad (2)$$

Two quantities, Q_{11} and Q_{12} , determine $\hat{\mathbf{Q}}$, thus the order parameter, $\mathbf{Q} \equiv \langle \hat{\mathbf{Q}} \rangle$, can be rewritten as an amplitude and phase, $Qe^{2i\theta}$. For a nonzero order parameter, the Fermi surface becomes elliptical, reflecting the broken symmetry of the nematic phase.

In the spirit of Ginzburg-Landau theory, the free energy of the ground-state is written as

$$F(\mathbf{Q}) = F(\mathbf{0}) + \frac{A}{4} \text{Tr}[\mathbf{Q}^2] + \frac{B}{8} \text{Tr}[\mathbf{Q}^4] + \dots \quad (3)$$

The odd terms have been dropped because \mathbf{Q} is odd under 90° rotations. Thus, positive A gives rise to an isotropic state ($\mathbf{Q} = 0$), and negative A gives rise to the nematic state, at which point $\mathbf{Q} = \sqrt{|A|/B}$.

Oganessian *et al.* consider a microscopic model in order to demonstrate that such an isotropic-to-nematic transition can exist. The Hamiltonian is taken to be

$$H = \int d\mathbf{r} \Psi^\dagger(\mathbf{r}) \epsilon(\vec{\nabla}) \Psi(\mathbf{r}) + \frac{1}{4} \int d\mathbf{r} \int d\mathbf{r}' F_2(\mathbf{r} - \mathbf{r}') \text{Tr}[\hat{\mathbf{Q}}(\mathbf{r}) \hat{\mathbf{Q}}(\mathbf{r}')], \quad (4)$$

with a single-particle energy

$$\epsilon(\mathbf{k}) = v_F q [1 + a(q/k_F)^2], \quad q \equiv |\mathbf{k}| - k_F, \quad (5)$$

and an interaction potential

$$F_2(\mathbf{r}) = \frac{1}{(2\pi)^2} \int d\mathbf{k} e^{i\mathbf{q}\cdot\mathbf{r}} \frac{F_2}{1 + \kappa F_2 q^2}. \quad (6)$$

Within this model, Oganessian *et al.* obtain the result that

$$A = \frac{1}{2N_F} + F_2, \quad B = \frac{3aN_F|F_2|^3}{8(v_F k_F)^2}, \quad (7)$$

where N_F is the density of states at the Fermi surface. By showing that F_2 can be both sufficiently large and negative, Oganessian *et al.* confirm that the coefficient A can indeed be negative within this model, resulting in a nonzero order parameter and driving the system into a nematic state.

An alternative mechanism for realizing a nematic state is the melting of striped state [3, 6]. Striped phases can arise in many condensed matter systems from the competition between short-range, attractive interactions and long-range, repulsive interactions [6]. If translational symmetry can be restored from the striped state while maintaining the broken rotational symmetry, a nematic phase occurs.

For example, Fradkin and Kivelson developed a theory showing this to be the case in certain quantum Hall systems: Quantum fluctuations may be too small to break local orientational order but large enough to restore translation symmetry [6]. A qualitative phase diagram for a quantum Hall system that includes this stripe-to-nematic transition is shown in Figure (2) along with a representation of both mechanisms for the formation of nematic phases.

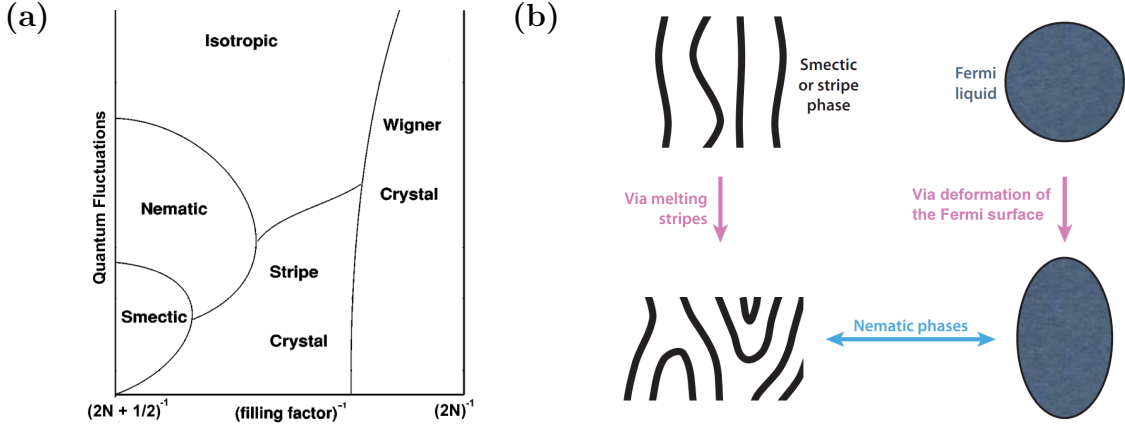


Figure 2. (a) A qualitative phase diagram for a two-dimensional electron gas at zero temperature. Quantum fluctuations increase along the vertical axis, while the inverse filling factor of the highest spin-polarized Landau level, N , is measured along the horizontal axis. (Figure modified from [6].) (b) Representations of the two mechanisms behind nematic phases. The left shows the partial melting of a stripe phase; the right represents the deformation of the Fermi surface. (Figure modified from [3].)

In order to fully characterize the QLC nematic, some crucial properties are listed in [3] as follows:

1. The QLC nematic state exhibits the same broken rotational symmetry as a classical nematic. This symmetry-breaking is reflected by anisotropic transport within a nematic sample.
2. The Goldstone modes are overdamped throughout the nematic phase for continuum systems except along specific, symmetry-determined directions. These overdamped Goldstone modes mark the breakdown of Fermi liquid theory [5].
3. The Goldstone modes become gapped in the presence of a lattice, suppressing non-Fermi liquid behavior. Near the quantum phase transition, however, the lattice effects are negligible, and non-Fermi liquid behavior is still observed.

2.2.2 Smectic phases

QLC smectic phases are also possible, such as in the two-dimensional electron gas of Figure 2. These phases are very similar to the striped phases referenced in Sec. 2.2.1 with the crucial

difference that smectic phases are conducting, whereas striped phases are insulating [6, 7, 8]. The striped order serves as the layered order of smectics, breaking rotational and translational symmetry, while the electrons remain able to move throughout the sample. Smectic phases typically consist of density wave states, such as charge density waves [3, 7].

To close this discussion of the electronic extension of liquid crystal theory, a comparison of a classical liquid crystal phase diagram and proposed QLC phase diagram is presented in Figure 3. The qualitative diagrams show how both classes of systems could progress from crystal to smectic (or striped) to nematic phases, followed by (Fermi) liquid and (Fermi) gas phases.

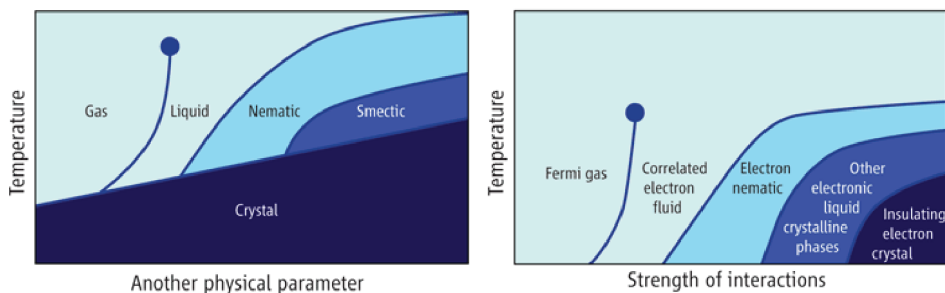


Figure 3. The diagram on the left is a possible phase diagram for a classical liquid crystal. The diagram on the right is a proposed phase diagram including quantum liquid crystal states. The “other electronic liquid crystalline phases” could include striped or smectic order. (Figure modified from [2].)

3 Experimental evidence for quantum liquid crystals

3.1 Quantum Hall system, GaAs/GaAlAs

The first definitive experimental demonstration of QLC phases appeared in quantum Hall heterojunctions in GaAs/GaAlAs and was presented in [9] and [10]. The QLC theory specific to quantum Hall systems was developed in [6].

Because QLC phases must arise out of spontaneously broken symmetries, great care was taken to produce clean and homogeneous samples. The samples presented were rotated during growth in order to guarantee good homogeneity, and the samples were demonstrated to be especially clean [9].

Figure 4 contains two plots of the anisotropic resistance observed in these systems. The first panel of Figure 4 contains two sets of data from a single sample, labeled sample *A*. The two sets were taken with the current in different directions through the sample, as pictured in the figure. The higher Landau levels show a marked resistivity anisotropy. Lilly *et al.* note that normalization between the two datasets was necessary due to irregularities in the contact positions on the sample. Thus, the solid curve was multiplied by 0.62 so as to match the low-field data. This is common practice when measuring resistances in quantum Hall systems [9]. Even without the correction factor, the anisotropic resistance is evident with

a ratio of nearly 100 at $\nu = 9/2$. The anisotropy was only present for temperatures below 150 mK and Landau levels $N > 1$ [9].

The second panel of Figure 4 shows similar data for two samples, *B* and *C*, taken from the same wafer as *A*. By cutting the samples into Hall bars, the current paths in the samples could be better defined [9]. Though less pronounced between *B* and *C*, the same anisotropy is seen as in sample *A*. Note that a normalization factor of 0.75 was applied to the data from sample *C*.

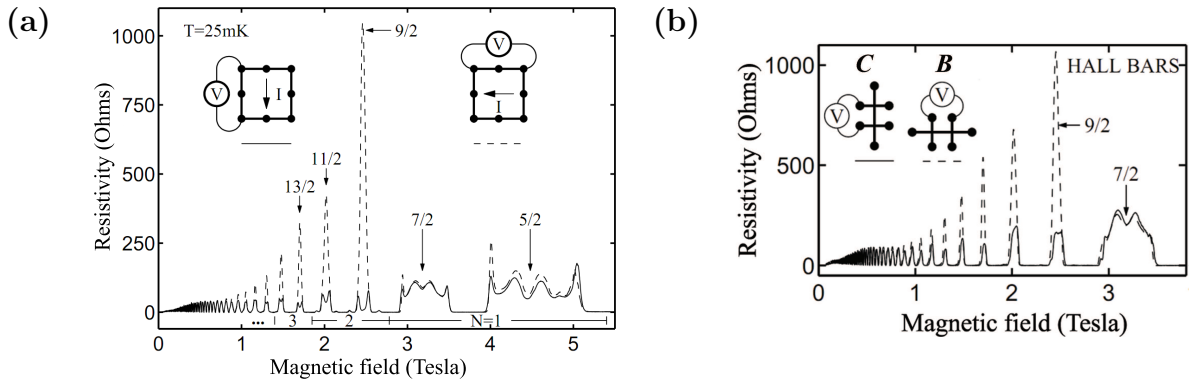


Figure 4. (a) Resistivity data from sample *A* of [9]. The two directions of current demonstrate a strong anisotropy. The solid curve was multiplied by a factor of 0.62 to normalize the datasets into agreement at very low fields. (b) Resistivity data from samples *B* and *C* of [9]. These Hall bar samples from the same wafer exhibit a similar (though weaker) anisotropy as sample *A*. The solid curve was multiplied by a factor of 0.75. (Figure modified from [9].)

An early interpretation of this anisotropic resistivity was the existence of a QLC phase in this two-dimensional electron gas system [6]. A basic description for a smectic phase at $T = 0$ is as follows: For a filling factor, ν , that is globally between full-filling, N , and half-filling, $N + 1/2$, the sample will separate into alternating regions of $\nu = N$ and $\nu = N + 1$. (Note that the case of full-filling, $N + 1$, and half-filling, $N + 1/2$, is equivalent.) As the global filling factor approaches N and the $\nu = N + 1$ regions decrease in size, the edge states surrounding the $\nu = N + 1$ regions eventually couple. This coupling produces stripe ordered charge density wave states that separate the $\nu = N$ regions. Electronic transport along the stripes is expected to be high, while hopping between adjacent regions should be much harder.

By then accounting for the effects of quantum fluctuations, Fradkin and Kivelson conclude that a nematic phase should exist between the smectic and isotropic phases. While the resistivity in perpendicular directions should be equal at $T = 0$, Fradkin and Kivelson conclude that a preferred direction should arise above zero temperature. Thus, the rotationally asymmetric smectic and nematic phases can explain the anisotropic resistivity observed in the GaAs/GaAlAs system.

3.2 Strontium ruthenate, $\text{Sr}_3\text{Ru}_2\text{O}_7$

In 2007, Borzi *et al.* published remarkable data displaying an apparent electron nematic phase in ultra-high-quality crystals of the strontium ruthenate $\text{Sr}_3\text{Ru}_2\text{O}_7$ [11]. The structure of $\text{Sr}_3\text{Ru}_2\text{O}_7$ consists of weakly coupled two-dimensional layers such that conduction is high in the ab plane [3]. Figure 5 contains the crucial plots establishing a QLC nematic state in $\text{Sr}_3\text{Ru}_2\text{O}_7$.

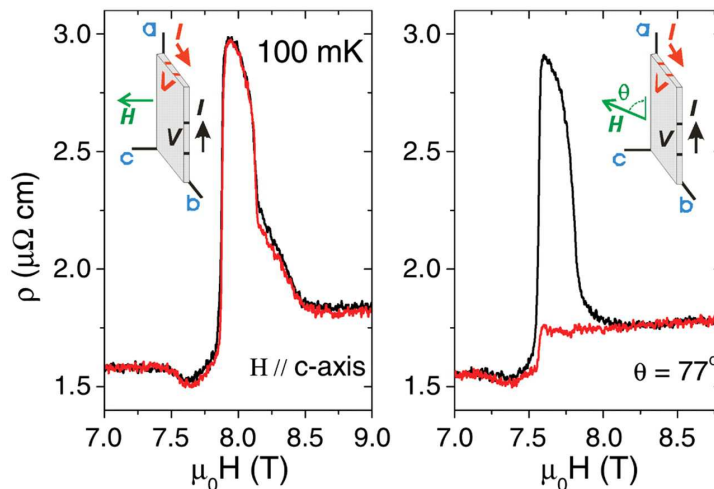


Figure 5. Measured resistivity of $\text{Sr}_3\text{Ru}_2\text{O}_7$ along the a - and b -directions in the presence of an applied magnetic field. With the magnetic applied perpendicular to the ab plane (to within 2°), the resistivity in both directions is nearly equal at the quantum critical point of ~ 7.8 T. When the applied field is tilted, however, the resistivity becomes highly anisotropic at the critical point, marking a nematic phase. (Figure modified from [11].)

The existence of a quantum critical point accessed by a magnetic field of ~ 7.8 T applied perpendicular to the ab plane had been well established prior to [11]. This critical point appears as a sharp spike in the resistivity in the a - and b -directions, as seen in the first panel of Figure 5. The steep slopes on either side of the quantum critical point mark first-order phase transitions [11].

Tilting the magnetic field partially into the ab plane, however, reveals an anisotropy of the state at the quantum critical point. While the increase in resistivity disappears in the direction perpendicular to the in-plane component of the magnetic field, the parallel resistivity retains the critical behavior.

Borzi *et al.* argue that while this anisotropy only appears in the presence of a symmetry-breaking magnetic field, the state at the critical point is in fact a nematic state with spontaneously broken symmetry. With no in-plane component of the magnetic field, $\text{Sr}_3\text{Ru}_2\text{O}_7$ may break into randomly aligned anisotropic domains. The magnetic field then would not be the true mechanism behind the broken symmetry, but instead a mechanism for aligning the numerous domains, causing the bulk to reflect the broken symmetry of the quantum phase. This theory is supported by susceptibility and neutron scattering data [11].

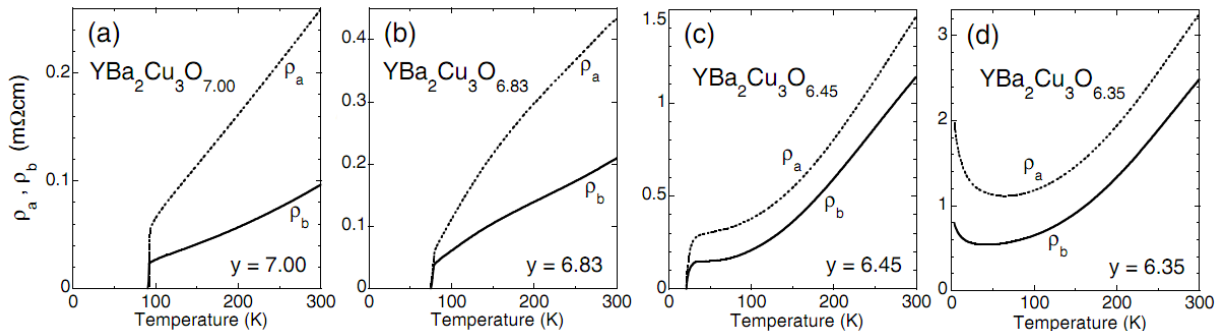


Figure 6. Resistivity measurements in YBCO along the a - and b -directions for four levels of doping. Panels (a)-(c) show a decrease in transport anisotropy, which follows the decreased orthorhombicity of YBCO at lower doping. Panel (d) then shows an increase in transport anisotropy despite lower doping and orthorhombicity, supporting the notion of a nematic phase in YBCO. (Figure modified from [12].)

This nematic phase in $\text{Sr}_3\text{Ru}_2\text{O}_7$ shares many similarities with the quantum Hall system discussed in Sec. 3.1 [11]. The apparent nematic phases in both are highly sensitive to temperature and sample purity, and in both cases, an in-plane field dictates an “easy” transport direction along with a perpendicular “hard” direction.

3.3 Cuprate superconductor, $\text{YBa}_2\text{Cu}_3\text{O}_{6+x}$

Probably the most exciting—as well as the most difficult—evidence for QLC phases was published in 2002 by Ando *et al.* [12]. The excitement stems from the fact that the system in question is the high- T_C superconductor $\text{YBa}_2\text{Cu}_3\text{O}_{6+x}$ (YBCO), the hope being that QLC phases may be able to illuminate some of the unsolved mysteries of high- T_C superconductivity, such as the pseudogap region. The difficulty posed by this material is that the orthorhombic structure (orthorhombicity up to 1.7% [12]) of YBCO introduces an intrinsic anisotropy, which could generate the same anisotropic electron transport attributed to QLC phases. Despite this difficulty, strong evidence suggests QLC phases exist in YBCO.

The first datasets suggesting a QLC state in YBCO are shown in Figure 6. The plots show the temperature dependence of the resistivity in the a - and b -directions for four different levels of doping of $\text{YBa}_2\text{Cu}_3\text{O}_{6+x}$ ($x = 1.00, 0.83, 0.45$, and 0.35). From panels (a)-(c), a clear trend is apparent that as doping decreases, the transport anisotropy also decreases. This is expected given that the orthorhombicity of YBCO also decreases with decreased doping, i.e., the intrinsic anisotropy is lowered with decreased doping. Between panels (c) and (d), however, the transport anisotropy suddenly increases. This increase obviously could not be due to the orthorhombic structure.

Figure 7 is a color map of the anisotropic transport ratio generated from data for 12 levels of doping. Decreasing anisotropy can be seen from $x = 1.0$ to $x = 0.6$. The anisotropy ratio then increases to ~ 2.5 for $x = 0.35$ where the orthorhombicity is only 0.26% [12].

The case for QLC phases in YBCO was strengthened in 2008 by neutron-scattering experiments with $\text{YBa}_2\text{Cu}_3\text{O}_{6.45}$ [13]. Hinkov *et al.* concluded that YBCO exhibits an

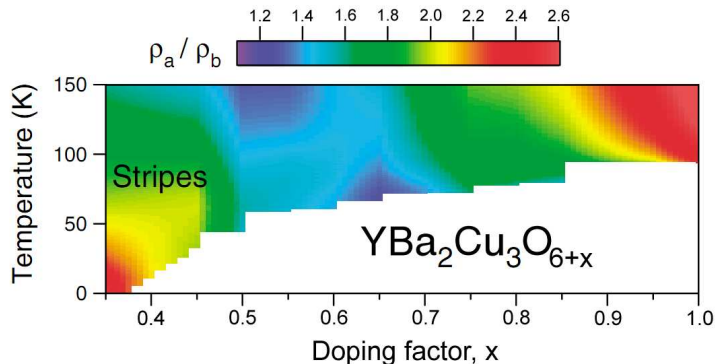


Figure 7. Color map of transport anisotropy in YBCO at various doping levels and temperatures. The map was generated from data from 12 levels of doping. The white region indicates the superconducting regime. Increased anisotropy below $x \approx 0.66$ supports a nematic phase in YBCO. (Figure modified from [12].)

instability to form uniaxial spin domains below $T = 150$ K. The orthorhombicity of the crystal then serves only to align the domains, much like the in-plane field component in $\text{Sr}_3\text{Ru}_2\text{O}_7$. Hinkov *et al.* note that the neutron scattering data is in close agreement with the proposed nematic phase’s dependence on temperature and doping demonstrated by [12]. Thus, as evidence for a nematic phase in YBCO mounts, the relevance of QLC phases to the pseudogap must be seriously considered.

4 Quantum liquid crystals in ultracold gases

Recent proposals have suggested that QLC phases may be accessible and modeled in ultracold atomic or molecular dipolar gases. Such systems can provide very pure, highly controllable environments to explore the nature of QLC phases and transitions. Three possibilities are discussed briefly below, two on optical lattices [14, 15] and one in continuum [16].

Quintanilla *et al.* propose that dipolar fermions in an optical lattice can provide a model of for a smectic phase, provided a bias field eliminates dipolar interactions in one direction. Because the dipole-dipole interaction is proportional to $[1 - 3 \cos^2 \theta]$, where θ is the angle between the two adjacent dipoles and their alignment, a strong bias field applied at $\theta = 54.736^\circ$ will extinguish the dipole-dipole interactions along one direction of the lattice. This creates a smectic order with only inter-chain dipole-dipole interactions left in the system. The proposed configuration can be seen in Figure 8.

While the lattice considered by Quintanilla *et al.* is fundamentally anisotropic due to the bias field, QLC phases in isotropic lattices have also been proposed [15]. In this case, the external bias field is applied perpendicular to the optical lattice such that any symmetries broken in the lattice plane would be spontaneous, potentially creating a true QLC nematic phase. Through both Hartree-Fock mean-field theory and linear-response analysis, Lin *et al.* determined that both nematic and smectic phases should be producible. The nematic phase could be probed with time-of-flight imaging, which measures the anisotropic expansion of

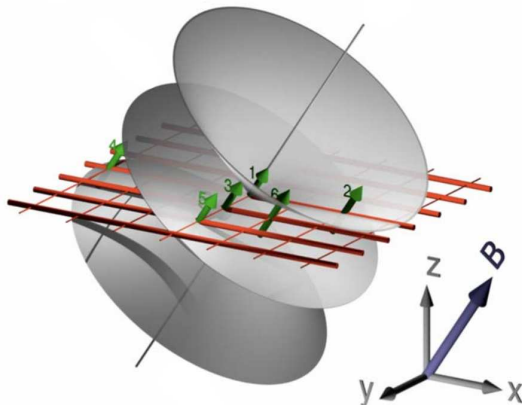


Figure 8. Proposed configuration for generating a state with smectic order in ultracold dipolar gases. The strong biasing field, B , at 54.736° with the x -axis extinguishes the dipole-dipole interactions in the x -direction, leaving only stripe interactions in the y -direction. (Figure modified from [14].)

the atomic cloud after release from the lattice.

Finally, Fregoso *et al.* propose that a nematic phase could be produced in an ultracold gas of fermions in the absence of a lattice. As with the previous two proposals, an external field is applied to the cloud, aligning the dipoles along a single direction. The resultant state has the same symmetry as a nematic, except that the rotational symmetry was not spontaneously broken. For strong enough fields, however, the rotational symmetry about the bias field could be spontaneously broken, creating a biaxial nematic phase. (A biaxial nematic phase maintains translational symmetry but has three distinct axes like a uniform ensemble of aligned rectangles [4].) The biaxial nematic state could be detected using polarized light scattering because in such a state the ultracold cloud should act as a birefringent medium [16].

5 Conclusions

The extension of liquid crystal phases to strongly correlated systems holds great potential. The demonstration of QLC phases in the quantum Hall system GaAs/GaAlAs and the strontium ruthenate $\text{Sr}_3\text{Ru}_2\text{O}_7$ bolster the field, while the evidence for such phases in YBCO promises exciting discoveries to come. As these symmetry breaking phases are better understood by theory and tested by experiments, QLC theory may be able to answer some of the most compelling unanswered questions in condensed matter physics, such as the pseudogap in high- T_C superconductors.

References

- [1] S. A. Kivelson, E. Fradkin, & V. J. Emery. “Electronic liquid-crystal phases of a doped Mott insulator.” *Nature* **393**, 550 (1998).
- [2] E. Fradkin, S. A. Kivelson, & V. Onanesyan. “Electron Nematic Phase in a Transition Metal Oxide.” *Science* **314**, 196 (2007).
- [3] E. Fradkin, S. A. Kivelson, M. J. Lawler, J. P. Eisenstein, & A. P. Mackenzie. “Nematic Fermi Fluids in Condensed Matter Physics.” *Annu. Rev. Condes. Matter Phys.* **1**, 153 (2010).
- [4] P. G. de Gennes & J. Prost. *The Physics of Liquid Crystals, 2nd Ed.* Clarendon Press (1993).
- [5] V. Oganessian, S. A. Kivelson, & E. Fradkin. “Quantum theory of a nematic Fermi fluid.” *Phys. Rev. B* **64**, 195109 (2001).
- [6] E. Fradkin & S. A. Kivelson. “Liquid-crystal phases of quantum Hall systems.” *Phys. Rev. B* **59**, 8065 (1999).
- [7] S. A. Kivelson, I. P. Bindloss, E. Fradkin, V. Oganessian, J. M. Tranquada, A. Kapitulnik, & C. Howald. “How to detect fluctuating stripes in the high-temperature superconductors.” *Rev. Mod. Phys.* **75**, 1201 (2003).
- [8] K. Sun, B. M. Fregoso, M. J. Lawler, & E. Fradkin. “Fluctuating stripes in strongly correlated electron systems and the nematic-smectic quantum phase transition.” *Phys. Rev. B* **78**, 85124 (2008).
- [9] M. P. Lilly, K. B. Cooper, J. P. Eisenstein, L. N. Pfeiffer, & K. W. West. “Evidence for an Anisotropic State of Two-Dimensional Electrons in High Landau Levels.” *Phys. Rev. Lett.* **82**, 394 (1999).
- [10] R. R. Du, D. C. Tsui, H. L. Stormer, L. N. Pfeiffer, K. W. Baldwin, & K. W. West. “Strongly anisotropic transport in higher two-dimensional Landau levels.” *Sol. St. Comm.* **109**, 389 (1999).
- [11] R. A. Borzi, S. A. Grigera, J. Farrell, R. S. Perry, S. J. S. Lister, S. L. Lee, D. A. Tennant, Y. Maeno, & A. P. Mackenzie. “Formation of a Nematic Fluid at High Fields in $\text{Sr}_3\text{Ru}_2\text{O}_7$.” *Science* **315**, 214 (2007).
- [12] Y. Ando, K. Segawa, S. Komiya, & A. N. Lavrov. “Electrical Resistivity Anisotropy from Self-Organized One Dimensionality in High-Temperature Superconductors.” *Phys. Rev. Lett.* **88**, 137005 (2002).
- [13] V. Hinkov, D. Haug, B. Fauqué, P. Bourges, Y. Sidis, A. Ivanov, C. Bernhard, C. T. Lin, & B. Keimer. “Electronic Liquid Crystal State in the High-Temperature Superconductor $\text{YBa}_2\text{Cu}_3\text{O}_{6.45}$.” *Science* **319**, 597 (2008).
- [14] J. Quintanilla, S. T. Carr, & J. J. Betouras. “Metanematic, smectic, and crystalline phases of dipolar fermions in an optical lattice.” *Phys. Rev. A* **79**, 31601 (2009).
- [15] C. Lin, E. Zhao, & W. V. Liu. “Liquid crystal phases in ultracold dipolar fermions on a lattice.” *Phys. Rev. B* **81**, 45115 (2010).
- [16] B. M. Fregoso, K. Sun, E. Fradkin, & B. L. Lev. “Biaxial nematic phases in ultracold dipolar Fermi gases.” *New Jour. Phys.* **11**, 103003 (2009).